

Interaction of reactive ions with Pt(100). II. Dissociative scattering of molecular ions near the threshold energy region

Housei Akazawa and Yoshitada Murata

Citation: *The Journal of Chemical Physics* **92**, 5560 (1990); doi: 10.1063/1.458489

View online: <http://dx.doi.org/10.1063/1.458489>

View Table of Contents: <http://scitation.aip.org/content/aip/journal/jcp/92/9?ver=pdfcov>

Published by the [AIP Publishing](#)

Articles you may be interested in

Chemistry of arsenic incorporation during GaAs/GaAs(100) molecular beam epitaxy probed by simultaneous laser flux monitoring and reflection highenergy electron diffraction

J. Vac. Sci. Technol. B **14**, 2742 (1996); 10.1116/1.589013

An analytical sixdimensional potential energy surface for dissociation of molecular hydrogen on Cu(100)

J. Chem. Phys. **104**, 7344 (1996); 10.1063/1.471402

Metal overlayers on organic functional groups of selforganized molecular assemblies. II. Xray photoelectron spectroscopy of interactions of Cu/CN on 12mercaptododecanenitrile

J. Vac. Sci. Technol. A **11**, 2382 (1993); 10.1116/1.578338

Potentialenergy surfaces for Pt₂+H and Pt+H interactions

J. Chem. Phys. **92**, 541 (1990); 10.1063/1.458457

Compact pulsed molecular beam system for realtime reactive scattering from solid surfaces

Rev. Sci. Instrum. **58**, 1014 (1987); 10.1063/1.1139602



Interaction of reactive ions with Pt(100). II. Dissociative scattering of molecular ions near the threshold energy region

Housei Akazawa^{a)} and Yoshitada Murata

The Institute for Solid State Physics, The University of Tokyo, 7-22-1, Roppongi, Minato-ku, Tokyo 106, Japan

(Received 30 March 1989; accepted 11 January 1990)

Dissociative scattering of N_2^+ , CO^+ , and CO_2^+ ions from Pt(100) has been studied at low energies. For dissociated N^+ emergence, the threshold of incident kinetic energy was found to be 40 eV. The threshold of dissociated CO^+ emergence in the CO_2^+ incidence was clearly observed at 25 eV. The threshold of dissociated C^+ emergence in the CO^+ incidence was observed at 70 eV. Correlation between the dissociation energy of a free molecule and the threshold of incident kinetic energy is clearly discernible. The angular distributions show that the dissociation product appears at larger scattering angles than that for the parent molecular ions scattered nondissociatively. These experimental results are consistent with the model that dissociation is due to translational-rovibrational energy transfer above the dissociation limit at the impulse collision with the surface.

I. INTRODUCTION

Dissociation of molecules on a surface has fundamental importance in the fields of molecular physics and surface science. Dissociation is an elementary step in chemical reactions on the surface. Surface-catalyzed dissociation of small molecules frequently proceeds with a sizable activation barrier. This barrier is, at most, lower than the dissociation energy of the free molecule. A seeded supersonic molecular beam with variable kinetic energy has enabled a well-controlled experiment which could not be attained by dosing ambient gas.¹ Activated dissociative chemisorption, with an activation barrier less than about 3 eV, has been studied by many groups, whereas dissociatively scattered products have scarcely been measured by experiments of molecular beam scattering.

Dissociative scattering of diatomic molecules has been studied traditionally with a molecular ion beam at much higher energies than the usual energy of neutral beams. The energy of the low-energy ion beams commonly used in surface science, above 100–200 eV, is much higher than the dissociation energy of free molecules, 1–10 eV, but it has been shown that a substantial amount of molecular ions (or neutrals) survive without dissociation.^{2–5} However, other processes such as sputtering, defect formation, and secondary-ion emission take place by bombarding the surface with an ion beam of this energy range, and these processes confuse the phenomenon of interest. In addition, the beam flux of ions is low in comparison with the molecular beam. Therefore, it is difficult to study the dynamics and the mechanism of reaction (dissociative chemisorption) clearly using such an ion beam. Dissociative chemisorption and scattering of fragments are outcomes from the dissociation process. To search for the branching between the two processes, it is important to understand the dissociation process by the use of an ion beam of lower energy for studying microscopic

parameters such as orientation of the molecular axis to the surface at impact.^{6–8}

Several models have been proposed to explain dissociative scattering in the hyperthermal energy range. These models are classified into electronic excitation and energy-transfer mechanisms. The electronic-excitation mechanism comes into play only when reactive intermediate species participate, and the dissociation threshold of the incident kinetic energy is lower than the dissociation energy of the ground-state molecule (ion). On the other hand, an incident molecule is translationally activated in the energy transfer mechanism. This process can be applied to all the species, and the dissociation threshold correlates with the dissociation energy of the incident molecule.

Snowdon, Heiland, and coworkers^{5,9–14} proposed a model of dissociative electron attachment. An incoming molecular ion to the surface can be neutralized to an electronically excited state by capturing an electron from the valence band of the metal. If this state is an antibonding state or a predissociation state, the molecule is dissociated without or with a low activation barrier. In the H_2^+ , N_2^+ , and O_2^+ scattering at grazing angle ($< 5^\circ$ from the surface) incidence on Ni(111),^{11–14} this model has been found to explain the relative kinetic energy distribution of the dissociation fragment. At sufficiently high energy where normal energy exceeds the dissociation energy, the mechanical energy transfer appears to dominate the interaction, causing dissociation via rotational and vibrational excitation.¹¹

The chemisorption interaction between the surface and constituent atoms of a molecule leads to dissociative chemisorption. If the molecule falls temporarily into a chemical interaction potential well in the vicinity of the surface but carries energy sufficient to surmount the attractive potential, the molecule can be dissociatively scattered. This is another electronic mechanism due to the catalytic effect of the surface. Gadzuk *et al.*^{15–18} proposed a dissociation mechanism due to the harpooning process, i.e., the transfer of translational to vibrational energy via the temporal formation of a negative molecular ion. Depending on the detail of

^{a)} Present address: NTT LSI Laboratories, 3-1, Morinosato Wakamiya, Atsugi 243-01, Japan.

the trajectory on the potential surface, the molecule is either dissociatively chemisorbed, vibrationally excited, or dissociatively scattered. Indeed, Haochang *et al.*¹⁹ observed the negative ion formation in scattering experiments of (100–300 eV)-O₂⁺ incidence on Ag(111) at θ_i (incidence angle measured from the surface normal) = θ_f (emission angle measured from the surface normal) = 20°. A similar experiment was performed by Reijnen *et al.*²⁰ at $\theta_i = \theta_f = 5^\circ$. Schubert *et al.*²¹ observed the O₂⁻ and CO₂⁻ formation on Ni(110) by impingement of O₂⁺ and CO₂⁺, respectively. Very recently, Danon and Amirav²² observed the I₂ formation in hyperthermal (1–12 eV)-I₂ beam scattering from a diamond (111) surface. However, clear verification of vibrational excitation or dissociative chemisorption mediated by the intermediate negative ion formation has not been reported.

The energy transfer mechanism is a translational-rovibrational energy transfer. From a difference in the geometrical (orientational) conditions of impact to the surface or from that in theoretical treatments, several models have been proposed. Bitensky and Parilis^{23,24} presented a theory of dissociative and nondissociative scattering of a diatomic homonuclear molecule based on classical trajectories. A mutual collision of constituent atoms with a flat surface is considered by maintaining a nearly parallel orientation to the surface. The condition required for the molecule escaping from dissociation is that the relative kinetic energy after collision is below the dissociation energy. Experimental results of 30 keV N₂⁺ scattering from Cu(100) at grazing incidence^{3,4} were explained by this model.²⁵

Gerber and Elber^{26–29} proposed a theory of dissociative scattering based on the idea that molecular dissociation in impulse collisions with the surface took place mainly by rotational predissociation. Upon impact on the surface, a rotational torque works as a centrifugal force on the molecule. If it is large enough to break the chemical bond, constituent atoms can be separated infinitely, surmounting the centrifugal barrier. Experimental results of dissociative scattering of (1–10 eV) I₂ from sapphire and MgO(100)^{30,31} were explained by their theory. It was demonstrated that I₂ could be dissociated at beam energies around the gas phase dissociation energy of the molecule.

In ion-molecule scattering, dissociation is usually treated by the spectator model, i.e., the translational-vibrational energy transfer above the dissociation limit in a collinear collision^{32–35}; scattering occurs in one of the atoms while the other does not participate in the scattering process. However, a vibrational excitation model has not been proposed explicitly for dissociative scattering of molecules (molecular ions) from solid surfaces. Classical trajectory calculations³⁶ of O₂ scattering from Ag(111) at energies of 100–300 eV revealed that the O⁻ formation in the experiment by the FOM group¹⁹ was entirely due to the impulse interaction. The geometrical condition leading to dissociation is that only one atom in the molecule is pushed against the repulsive potential of the surface. This dissociation process is similar to bond breaking due to vibrational excitation, rather than rotational excitation.

The present paper reports on dissociative scattering of N₂⁺, CO⁺, and CO₂⁺ from a Pt(100) surface near the threshold energy region (10–400 eV). This energy is the intermediate region between usual studies of dissociative scattering and dissociative chemisorption. From the energy dependence of the scattered ion yield and the angular distribution, the dissociation mechanism is discussed in terms of the translational-rovibrational energy transfer.

II. EXPERIMENT

The experimental apparatus and the method have been described previously.^{37,38} Scattered ions were detected with a rotatable quadrupole mass filter, without energy analysis. Trajectories of transmitted ions were bent 90° using a deflector, before detection with an electron multiplier. The energy of the dissociation product is determined from the mass ratio of the product ion to the parent molecular ion. The dissociation product of N₂⁺ ion, distinguished from the scattered N⁺ ion in the N⁺ incidence, N_{dis}⁺ carries about half of the energy of N₂⁺. The product C_{dis}⁺ carries about 0.429 of the energy of scattered CO⁺ and so on. Voltage applied to the deflector was adjusted for the measurement of each ion species.

Typical mass spectra of the scattered ions for molecular-ion incidence are shown in Fig. 1. In the incidence of the N₂⁺ ions, dissociatively scattered N_{dis}⁺ ions and nondissociatively scattered N₂⁺ ions were detected. In the incidence of O₂⁺ ions, only the O₂⁺ ions were detected but O_{dis}⁺ ions were not observed, probably due to their very low ion survival probability. In the incidence of the CO⁺ ions, both C_{dis}⁺ and CO⁺

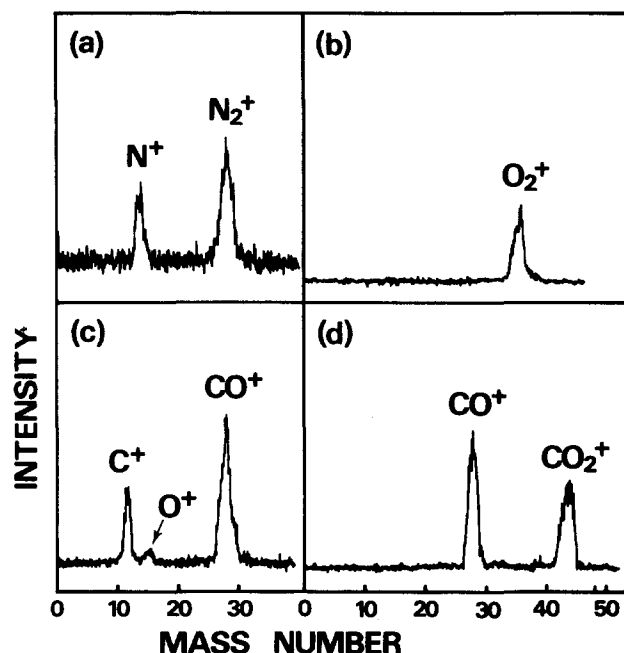


FIG. 1. Typical mass spectra showing dissociative scattering of (a) N₂⁺, (b) O₂⁺, (c) CO⁺, and (d) CO₂⁺ ions from a Pt(100) surface. Incident energies were 200 eV for N₂⁺, 50 eV for O₂⁺, 200 eV for CO⁺, and 100 eV for CO₂⁺.

were detected. When the incident energy was increased above 200 eV, a small amount of the O_{dis}^+ ions were detected. In the CO_2^+ incidence, both CO_{dis}^+ and CO_2^+ were detected but no O_{dis}^+ was detected.

The above observations can be compared with results of a similar experiment observing the negative ions scattered from a Ni(110) surface at a grazing incidence of 5° .²¹ In the CO^+ incidence, O_{dis}^- was detected but C_{dis}^- was not detected. In the CO_2^+ incidence, both O_{dis}^- and CO_2^- were detected but no CO_{dis}^- was detected. It should be noted that not all the species were observed when only positive or negative ions were detected. The appearance of these species depends on the electronic structure of the molecule.

III. RESULTS AND DISCUSSION

The dissociative scattering of an AB^+ -molecular ion forming the detectable product ion A_{dis}^+ is observed when species B is more electronically negative than A and A^+ has a sufficient survival probability. The positive charge of AB^+ is carried away by A_{dis}^+ . The ion yield of AB^+ and A_{dis}^+ in the AB^+ incidence and that of A^+ in the A^+ incidence were measured. The scattered ion yields of A^+ , A_{dis}^+ , and AB^+ are denoted by I_1 , I_{1d} , and I_2 , respectively. The three-stage model shows charge exchange between the projectile and the surface (Fig. 2). In this model, the ion-surface interaction region is divided into three parts: the incoming trajectory, the collision region, and the outgoing trajectory. Resonance neutralization, Auger neutralization, and Auger de-excitation take place on the incoming and the outgoing trajectory. Actually, almost 99% of the ions are neutralized on the incoming trajectory and de-excited to the ground state. In the collision region, the molecular orbital of the projectile and the atomic orbital of the target are merged into a molecular orbital of a quasimolecule.^{39,40} Electrons can be promoted to a highly excited state and collisional neutralization or reionization takes place. The ion yields are expressed as

$$I_1 = \sigma_1 P_1^{out} [P_1^{in} P_1^N + (1 - P_1^{in}) P_1^I], \quad (1)$$

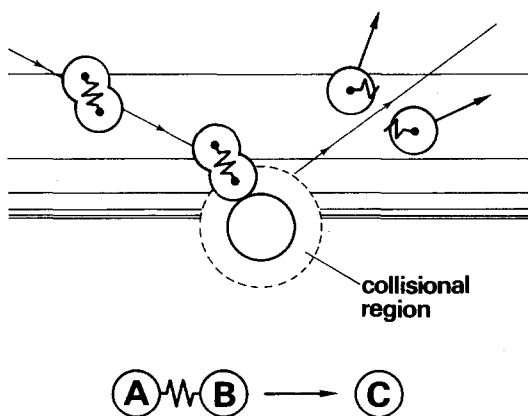


FIG. 2. Schematic explanation of a three-stage model and the dissociative scattering process of a diatomic molecular ion. Collinear collision of an AB molecule with C atom is also shown.

$$I_{1d} = \sigma_{1d} P_1^{out} [P_2^{in} P_2^N + (1 - P_2^{in}) P_2^I] P_{dis}, \quad (2)$$

$$I_2 = \sigma_2 P_2^{out} [P_2^{in} P_2^N + (1 - P_2^{in}) P_2^I] (1 - P_{dis}), \quad (3)$$

where σ_i is the effective differential cross section for scattering in a given scattering geometry, P_i^{in} (P_i^{out}) is the ion survival probability on the incoming (outgoing) trajectory, P_i^N and P_i^I are the ion survival and the reionization probabilities in the collision region, respectively. P_{dis} is the dissociation probability of AB^+ (AB). Subscripts 1, $1d$, and 2 correspond to A^+ , A_{dis}^+ , and AB^+ ion species, respectively. Constant factors, such as the number of the scattering centers on the surface and the detection efficiencies, are included in σ_i . Dissociation is assumed to take place from the ground state of N_2^+ or N_2 in the collision region. At the threshold of the incident energy, E_{th} , I_{1d} becomes zero. If I_1 and I_2 take significant values (more than two orders of magnitude larger than I_{1d}) around E_{th} , this means that P_i^{out} and $[P_2^{in} P_2^N + (1 - P_2^{in}) P_2^I]$ take significant values around E_{th} . The σ_i values ($i = 1, 1d$, and 2) are expected to take comparable nonzero values. The threshold energy for the emergence of A_{dis}^+ should then be the threshold of P_{dis} .

A. Dissociative scattering of N_2^+

The yields of the scattered N_2^+ , N_{dis}^+ , and N^+ ions in the specular direction at $\theta_i = 60^\circ$ are shown in Fig. 3. This result

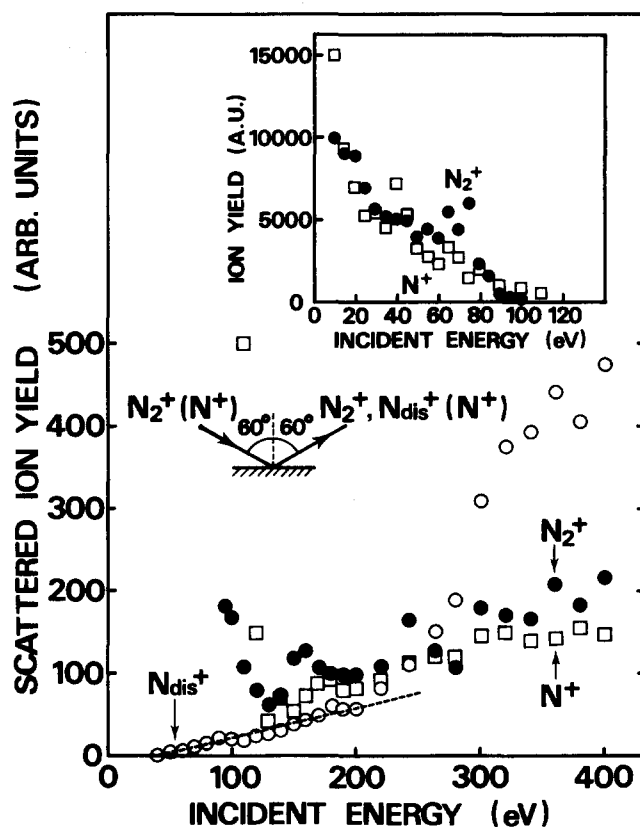


FIG. 3. Scattered ion yield as a function of incident energy for N_2^+ (solid circle) and N_{dis}^+ (open circle) in the N_2^+ incidence, and N^+ (open square) in the N^+ incidence. The incidence angle measured from the surface normal θ_i was 60° , and specularly scattered ions along the [001] azimuth were detected. Although the yield is given in arbitrary units, it is common to all figures in the present paper. The N_{dis}^+ data are fitted by the broken straight line. Inset shows the result in the region below 100 eV.

is similar to those with other incident angles $\theta_i = 50$ and 70° reported previously.³⁸ Since the N_{dis}^+ yield exhibits a linear dependence on the incident energy below 100 eV, the threshold energy for the N_{dis}^+ yield is concluded to be 40 eV. Since the yields of N_2^+ and N^+ are sufficiently large at 40 eV, according to the above argument, this threshold is also the dissociation threshold. The value of 40 eV is about four times as large as the dissociation energies for the ground state of N_2 (9.76 eV) and N_2^+ (8.72 eV).⁴¹ This observation is different from that of the low threshold energy nearly equal to the dissociation energy in the scattering of the iodine molecule.^{30,31} However, in the scattering of 1-iodopropane from diamond(111)⁴² the observed threshold, 3.7 eV, is higher than the dissociation energy, 2.3 eV. This threshold energy higher than the dissociation energy is similar to that observed in the present study.

The observed threshold energy is explained by accounting for the efficiency of the energy transfer. The translational-vibrational energy transfer at the impulse collision with a surface atom should be considered. The derivation of the threshold energy assumes collision of an AB molecule from an atom B onto a surface atom C collinearly keeping the molecular axis aligned to the moving direction (spectator model), as shown in Fig. 2. With this collision geometry, the translational energy is converted most efficiently to the vibrational energy of AB^+ (AB). It is also assumed that an AB^+ (AB) molecule is a harmonic or a Morse oscillator, initially at rest, and that the interaction between atoms B and C is purely repulsive, as expressed by the Born-Mayer potential. The second impact between atoms B and C can be neglected, and the vibrational energy gained at the first impact is assumed to be used totally for dissociation. Such a situation is realized if the collision is nearly collinear and the backscattered atom B passes the side of the spectator atom A . A reasonable analytical approximation for the energy transfer is known⁴³:

$$\delta E = 2(\pi\omega_0 L)^2 m m_C (m_A + m_B) \text{csch}^2(\pi\omega_0 L/v) \times \exp(-1.685m), \quad (4)$$

with $m = m_A m_C / [m_B (m_A + m_B + m_C)]$, where m_A , m_B , and m_C represent the masses of atoms A , B , and C , respectively, ω_0 is the resonance frequency of the oscillator, L is the scale length of the Born-Mayer potential, and v is the incident velocity of AB^+ (AB). This expression is applicable to small m , i.e. $m < 1$. AB^+ is assumed to be dissociated if δE exceeds the dissociation energy of AB^+ (AB). In the case of N_2^+ (N_2) collision on Pt, the dissociation energy is 8.72 eV (9.76 eV) and the threshold energy is 35 eV (38 eV), where parameters are $\omega_0 = 2207 \text{ cm}^{-1}$ (2359 cm^{-1}), $L = 0.274 \text{ \AA}$,⁴⁴ and $m = 0.8745$. These estimated threshold energies are in fair agreement with the observed values. Since there are some ambiguities in the above estimation, such as unknown vibrational excitation of the incident molecular ion (1–2 eV) and the choice of parameter L , we consider that this agreement is satisfactory.

Further support for the impulse collision model is obtained from the angular distribution. The angular distribu-

tions of N_2^+ and N_{dis}^+ at incident energies of 70, 100, 200, and 300 eV at $\theta_i = 60^\circ$ are shown in Figs. 4 and 5. At 70 eV, scattered N_2^+ emerges at 5° from the surface, whereas the distribution of N_{dis}^+ extends to large scattering angles and exhibits nearly a cosine distribution. At 100 eV, the lobe of N_2^+ is broadened slightly, but its maximum position is located at about 10° from the surface. The lobe of N_{dis}^+ still preserves a cosine-like feature but is directed to 50 – 60° from the surface. The angular distribution of N_{dis}^+ becomes more lobular with increasing energy. At 200 eV, the lobe of N_2^+ is located at 30° from the surface (in the specular direction) and that of N_{dis}^+ is located at 50° from the surface. At 300 eV, the scattering process becomes random and the angular distributions of N_2^+ and N_{dis}^+ spread to wider angles. The lobe of N_2^+ is located at 25° from the surface, and the lobe of N_{dis}^+ is located at 40° from the surface.

A common feature in the angular distributions observed at these energies is that the yield of N_{dis}^+ extends to wider scattering angles than that of N_2^+ and that the lobe position of N_{dis}^+ is located at a larger scattering angle than that of N_2^+ . This indicates that a smaller impact parameter is required for dissociative scattering than nondissociative scattering, since collision with a small impact parameter leads to large-angle scattering.

The possibility of other mechanisms should be considered by comparing the present data with other experimental results. Heiland *et al.* performed a time-of-flight measurement of (0.2–4.4 keV)- N_2^+ scattering at the grazing angle of incidence on Ni(111).^{9–11} The contents of the observed spe-

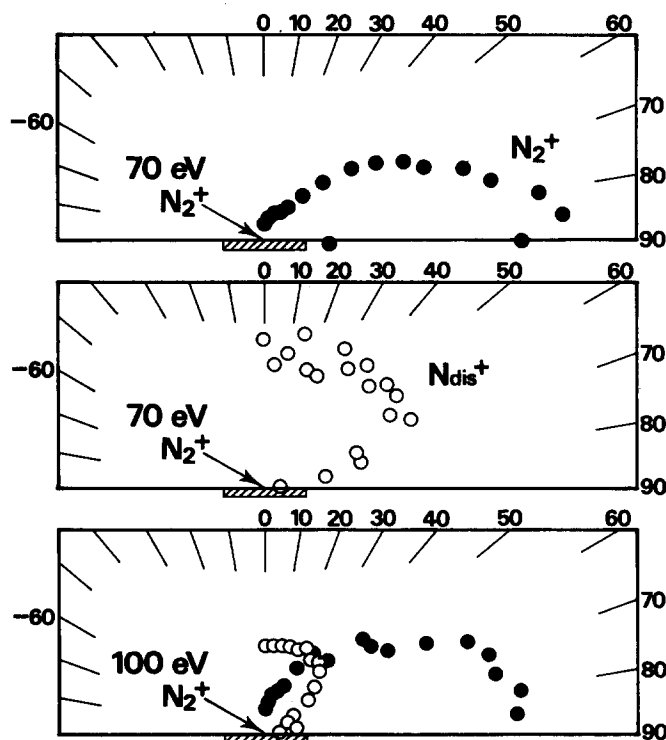


FIG. 4. Angular distribution of the scattered ions at 70 and 100 eV in the N_2^+ incidence with $\theta_i = 60^\circ$. Solid and open circles represent N_2^+ and N_{dis}^+ , respectively. The scale is arbitrary.

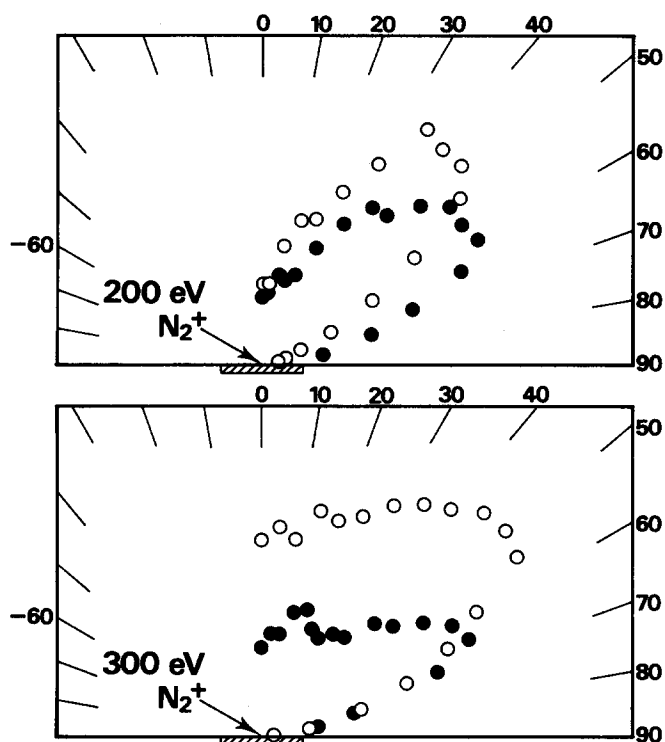


FIG. 5. Angular distribution of the scattered ions at 200 and 300 eV in the N_2^+ incidence with $\theta_i = 60^\circ$. Solid and open circles represent N_2^+ and N_{dis}^+ , respectively. The scale is arbitrary.

cies were about 90% of N_2 and 10% of N_{dis} below 1 keV. The ion yield was found to be less than 10^{-3} of the neutral yield. Resonance neutralization to $a^1\Pi_g$ or $B^3\Pi_g$, followed by the transition to a predissociation state of $^5\Sigma_g^+$, was invoked by them. Vibrational excitation required for the predissociation is $v = 6$ for $a^1\Pi_g$, and $v = 12$ for $B^3\Pi_g$, i.e., an activation barrier of 1–2 eV exists for predissociation. This condition is satisfied if the vibrational excitation of the primary beam is taken into account. Then, no actual activation barrier should be observed for this dissociation process, whereas the present experiment shows a high threshold energy of 40 eV. In addition, if dissociative attachment is the main contribution in dissociative scattering, the normal kinetic energy should be lower than the dissociation energy of N_2 or N_2^+ . Since the experimental condition is a grazing angle of incidence, $\psi_i = \psi_f = 5^\circ$, the normal kinetic energy is 7.6 eV at 1 keV incident energy, the limit for the dominant contribution of an electronic mechanism. A normal kinetic energy of 7.6 eV is well below the dissociation energies of N_2 and N_2^+ . However, the present experiment was carried out with an ordinary incident angle ($\theta_i = \theta_f = 50\text{--}70^\circ$). Thus, the mechanical model of the translational-vibrational energy transfer is very probably adequate. However, this model does not exclude the possibility of electronic dissociation, because this process is applicable to scattered neutrals which make up the dominant part of scattered particles. Ions were observed as only a small fraction of the scattered particles.

Sass and Rabalais⁴⁵ have studied scattering of N_2^+ in the 1.5–4.5 keV energy range from Au and graphite surfaces.

The relative kinetic energy distribution of the scattered atomic ions was obtained. Their interpretation of the experimental results was that dissociation occurs mainly from excited repulsive electronic states of the ion, which are achieved in impulse collision, rather than purely vibrational or rotational excitation from the ground state. A high kinetic energy is necessary for such an electronic excitation, and hence, this process is improbable for ions with the energy of tens of eV employed in the present experiment.

B. Dissociative scattering of CO^+

The scattered ion yield of C_{dis}^+ and CO^+ in the CO^+ incidence on the surface as a function of incident energy is shown in Figs. 6 and 7. For comparison, the yield of C^+ in the C^+ incidence is also shown in the figures. The measurement was performed at $\theta_i = 60$ and 70° with a specular scattering condition. A small amount of O_{dis}^+ was detected above 200 eV. Although the threshold is not clear, the signal of C_{dis}^+ starts at 70 eV. The yield then increases exponentially with energy. Since the energy dependences of the C^+ and C_{dis}^+ yields show a similar tendency, the exponential increase in the C_{dis}^+ yield, with around 200 eV as the onset, would be due to enhancement of the reionization process. At 400 eV, the yield of C_{dis}^+ is more than 10 times as large as that of nondissociatively scattered CO^+ , and the yield of C^+ is more than

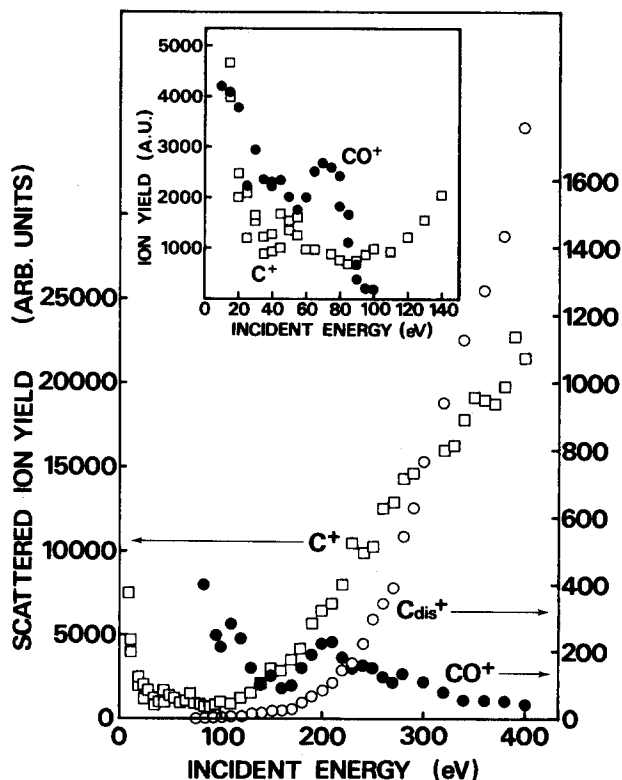
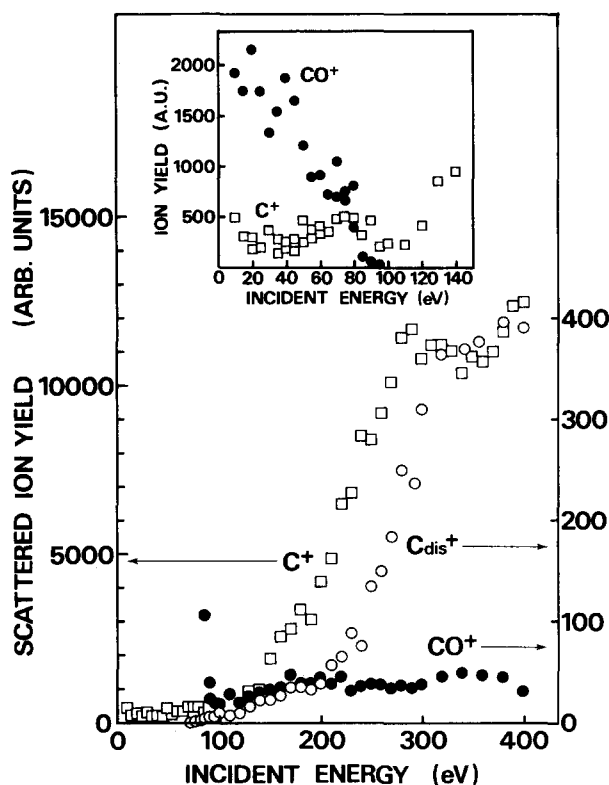


FIG. 6. Scattered ion yields as a function of incident energy for CO^+ (solid circle) and C_{dis}^+ (open circle) in the CO incidence, and C^+ (open square) in the C^+ incidence. The incidence angle θ_i was 70° and specularly scattered ions along the [001] azimuth were detected.

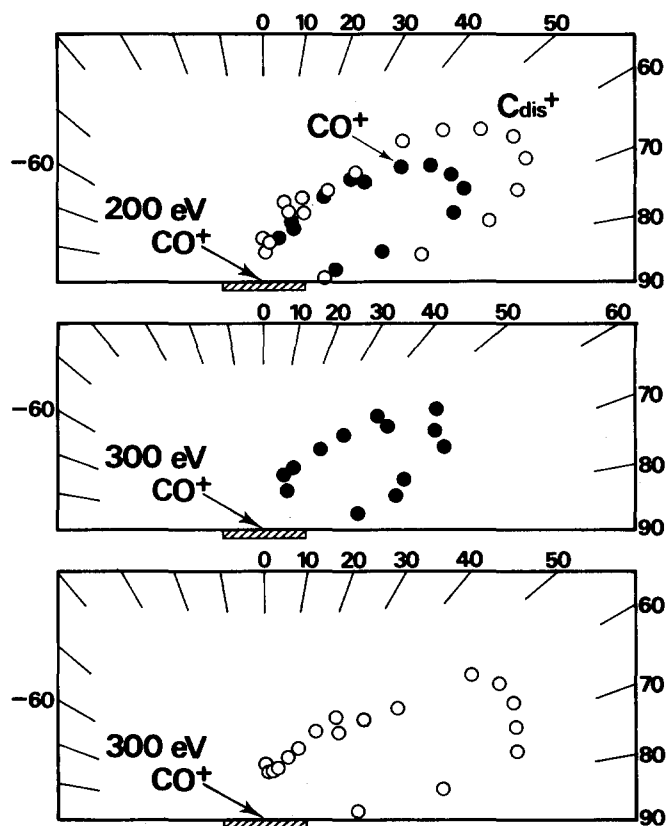
FIG. 7. Scattered ion yields at $\theta_i = 60^\circ$. See Fig. 6.

20 times as large as that of C_{dis}^+ . Since the CO molecule has no predissociation state below the Pt Fermi level accessible by resonance neutralization, a possible mechanism is the energy transfer mechanism.

The threshold energy of 70 eV may be explained similarly in the case of N_2^+ . The head-on collision from the oxygen atom to a Pt atom is considered. The atom A is carbon and the atom B is oxygen in Fig. 2. In such a collision, the carbon atom is far from the surface. This condition may be convenient for the survival of C_{dis}^+ . The dissociation energy of CO^+ (CO) is 8.34 eV (11.09 eV), and the corresponding threshold energy calculated from Eq. (4) is 28 eV (48 eV), where parameters are taken as $\omega_0 = 2170 \text{ cm}^{-1}$ (2214 cm^{-1}), $L = 0.2744 \text{ \AA}$,⁴⁴ and $m = 0.6558$. These energy values are smaller than the observed threshold of 70 eV. Therefore, dissociation from the ground state CO and subsequent reionization should be dominant contributions.

Jo *et al.*⁴⁶ reported dissociative scattering of CO^+ from a polycrystalline Mg surface. Peaks of nondissociatively scattered CO^+ in the energy spectra appeared always at the double-collision position, whereas peaks of dissociatively scattered C and O appeared at the single-collision position. Since the energy transfer in a double collision is smaller, a double collision is softer than a single collision if the scattering angles are the same. This supports the impulse collision model for dissociation.

The angular distributions of scattered C_{dis}^+ and CO^+ at $\theta_i = 60^\circ$ are shown in Fig. 8. The ion yield of C_{dis}^+ below 100 eV was not sufficient for measurement of the angular distri-

FIG. 8. Angular distributions of the scattered ions at 200 and 300 eV in the CO^+ incidence with $\theta_i = 60^\circ$. Solid and open circles represent CO^+ and C_{dis}^+ , respectively. The scale is arbitrary.

bution, and hence a similar discussion of dissociative scattering of N_2^+ near the threshold cannot be applied directly to that of CO^+ . The lobe positions of C_{dis}^+ and CO^+ are nearly identical above 200 eV, and are located in the specular direction. The angular distributions of C^+ at 200 and 300 eV in the C^+ incidence show a double-peak structure³⁷ and are considerably different from the angular distribution of C_{dis}^+ . No plausible speculation on the dissociation mechanism from the angular distribution can be made at this stage.

C. Dissociative scattering of CO_2^+

The scattered ion yields of CO_2^+ and CO_{dis}^+ in the specular direction as a function of incident energy are shown in Figs. 9 and 10. For comparison, the CO^+ yield in the CO^+ incidence is shown. Measurement was performed at two incidence angles of $\theta_i = 60$ and 70° . The CO_{dis}^+ signal starts at 25 eV, the yield increases steeply up to about 100 eV, and then increases slowly at $\theta_i = 70^\circ$ or saturates at $\theta_i = 60^\circ$. The yields of CO_2^+ and CO^+ generally decrease with increasing energy. Using the same analysis in the dissociative scattering of N_2^+ , described previously, the threshold kinetic energy of dissociation is 25 eV. The threshold energy of 25 eV is about five times as large as the dissociation energy of the ground state CO_2 molecule into $CO + O$ (5.453 eV). No predissociation states of CO_2 are known. Since CO_2 is a tria-

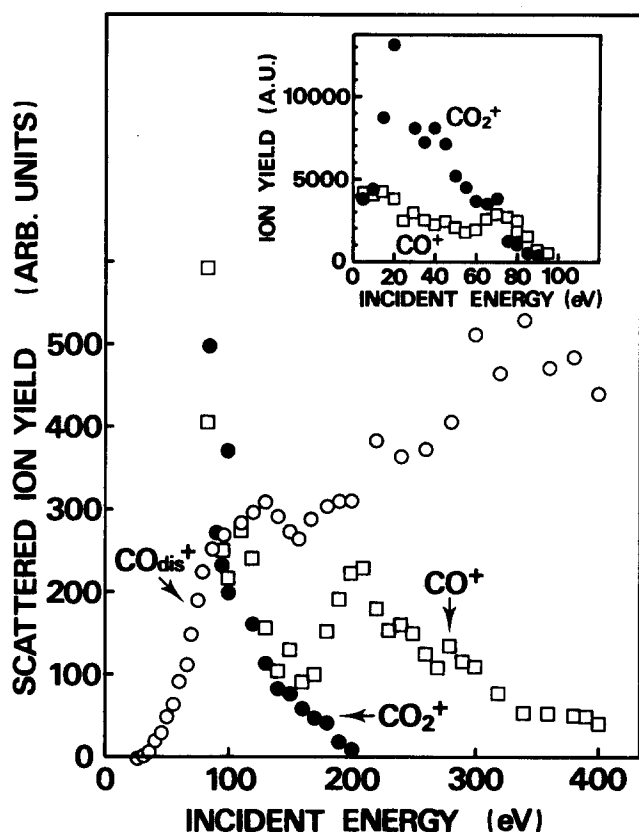


FIG. 9. Scattered ion yields as a function of incident energy for CO_2^+ (solid circle) and CO_{dis}^+ (open circle) in the CO_2^+ incidence, and CO^+ (open square) in the CO^+ incidence. The incidence angle θ_i was 70° and specularly scattered ions along the $[001]$ azimuth were detected. Inset shows the result in the region below 100 eV.

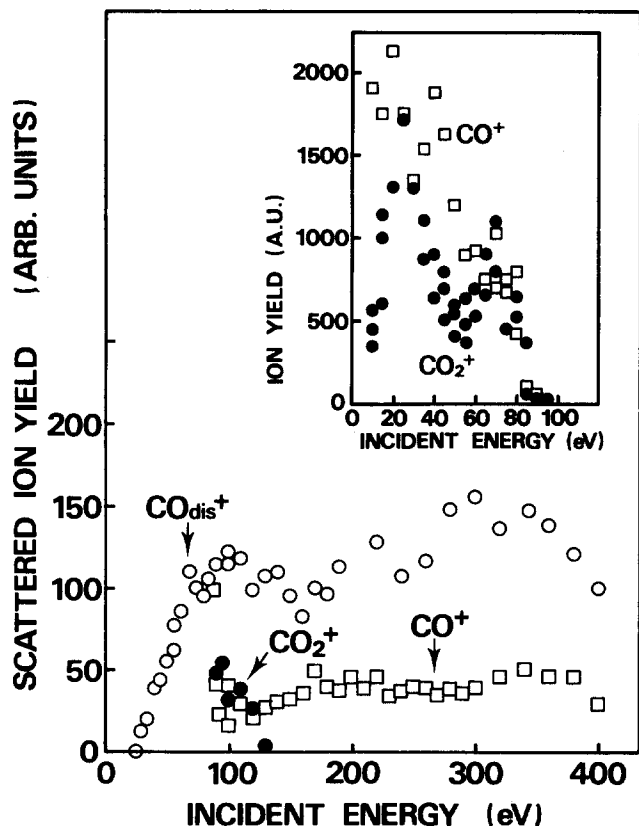


FIG. 10. Scattered ion yields at $\theta_i = 60^\circ$. See Fig. 9.

atomic molecule, it is not straightforward to obtain a quantitative relationship between the dissociation energy and the threshold energy, but there seems to be a correlation between the low threshold energy and the small dissociation energy. Schubert *et al.*²¹ indicated that bent CO_2^- species would be the intermediate leading to dissociation. In dissociation by the translational-rovibrational energy transfer, CO_2 may also be deformed significantly. In contrast, the activation barrier for dissociative chemisorption of CO_2 on $\text{Ni}(100)$ was found to be only 0.86 eV (83 kJ/mol) by a molecular beam experiment.⁴⁷

The angular distributions of scattered CO_{dis}^+ and CO_2^+ are shown in Figs. 11 and 12. At 50 eV, the lobe of CO_2^+ is located at $5\text{--}10^\circ$ from the surface, whereas that of CO_{dis}^+ is located at 20° from the surface. At 70 eV, the lobe of CO_2^+ is located at 10° from the surface and that of CO_{dis}^+ is located at 20° from the surface. At 100 eV, the lobe of CO_2^+ is located at 5° from the surface and that of CO_{dis}^+ is located at 15° from the surface. It is seen that the lobe position of CO_{dis}^+ appears always at a larger scattering angle than that of CO_2^+ . Since a smaller impact parameter is required for dis-

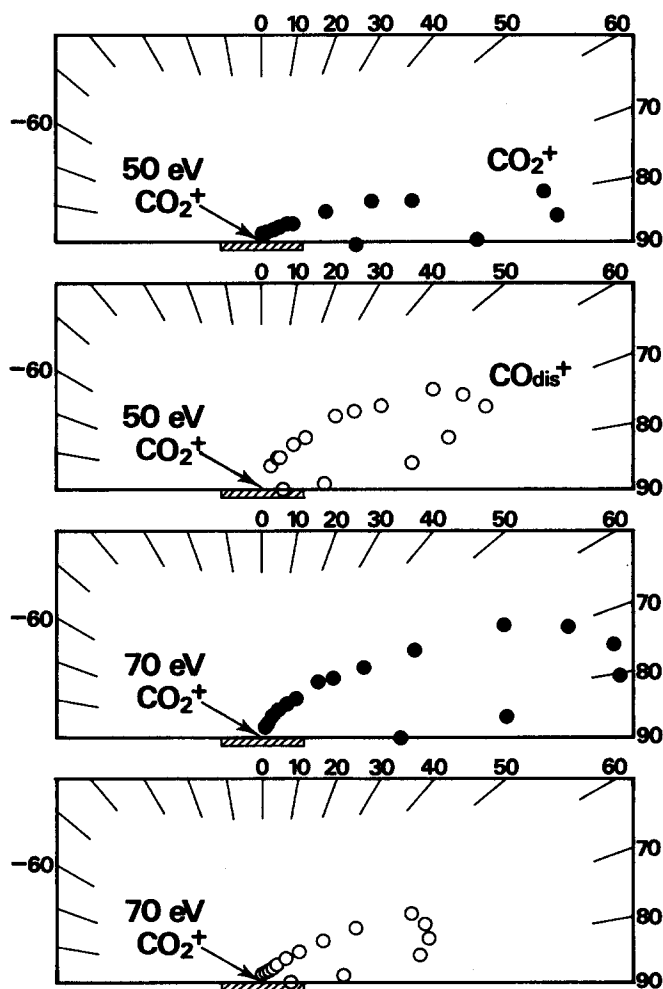


FIG. 11. Angular distributions of the scattered ions with 50 and 70 eV in the CO_2^+ incidence at $\theta_i = 60^\circ$. Solid and open circles represent CO_2^+ and CO_{dis}^+ , respectively. The scale is arbitrary.

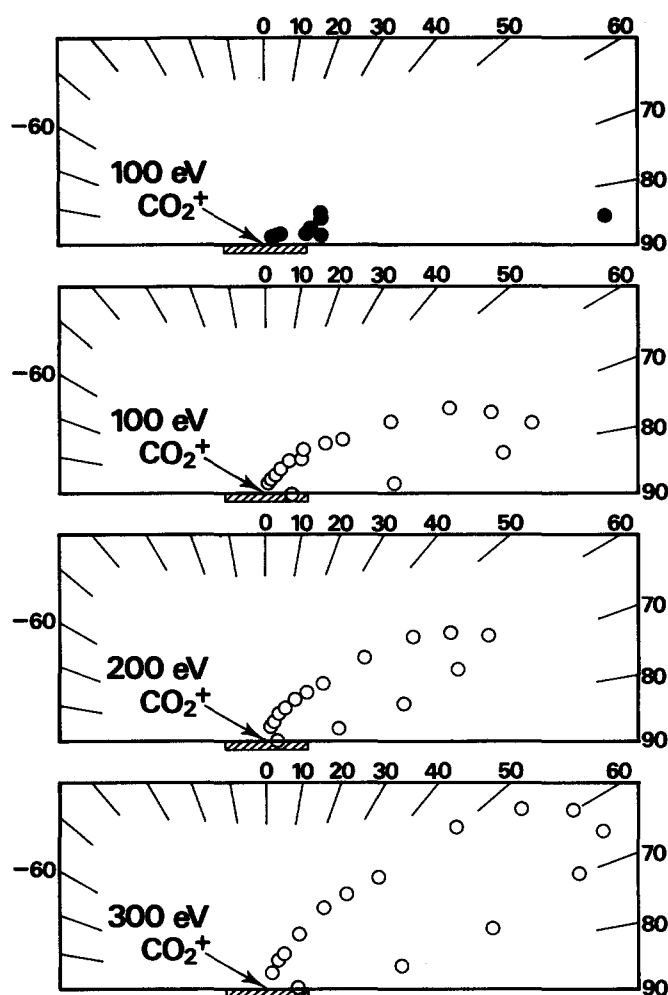


FIG. 12. Angular distributions of the scattered ions with 70, 100, 200, and 300 eV in the CO_2^+ incidence at $\theta_i = 60^\circ$. Solid and open circles represent CO_2^+ and CO^+ , respectively. The scale is arbitrary.

sociation, the dissociation mechanism of CO_2^+ will also be translational-rovibrational energy transfer in the impulse collision with the surface.

IV. SUMMARY

The dissociative scattering of N_2^+ , CO^+ , and CO_2^+ ions from a Pt(100) surface has been studied at the threshold energy region. The threshold of N^+ emergence in the N_2^+ incidence was found at 40 eV, that of C^+ emergence in the CO^+ incidence at 70 eV, and that of CO^+ emergence in the CO_2^+ incidence at 25 eV. There exists a correlation between the dissociation energy and the threshold incident energy. In the angular distribution of the scattered ions, dissociation product ions appear at larger scattering angles than those of the corresponding parent ions. These experimental results are explained by a model of the translational-vibrational energy transfer in the impulse collision with the surface.

In the present experiment, only the dissociatively scattered "ions" are detected. The threshold energy of this case can be explained by the model described above. If we could

detect dissociatively scattered neutral atoms or molecules, a lower threshold energy would have been observed, and the explanation would have needed other models. The survival probability of the dissociatively scattered ions is considered to be the highest in the collinear collision.

Dissociative chemisorption is characterized by low collision energy necessary for the reaction to proceed, below the dissociation energy of a free molecule, whereas dissociative scattering is characterized by high energy needed for dissociation. The effect of ion neutralization and spatial orientation of the molecular axis, which complicates the interpretation of the experimental results, must be treated properly. It is highly desirable to develop an oriented molecular beam of high kinetic energy.

ACKNOWLEDGMENTS

We thank Professor K. Kuchitsu for critically reading the manuscript. This work was financially supported by a Grant-in-Aid for Scientific Research from the Ministry of Education, Science, and Culture.

- ¹ J. A. Barker and D. J. Auerbach, *Surf. Sci. Rep.* **4**, 1 (1985).
- ² W. Eckstein, H. Verbeek, and S. Datz, *Appl. Phys. Lett.* **27**, 527 (1975).
- ³ L. L. Balashova, Sh. N. Garin, A. I. Dodonov, E. S. Mashkova, and V. A. Molchanov, *Surf. Sci.* **119**, L378 (1982).
- ⁴ L. L. Balashova, A. I. Dodonov, Sh. N. Garin, E. S. Mashkova, and V. A. Molchanov, *J. Phys. B* **16**, 2609 (1983).
- ⁵ W. Heiland, U. Beitz, and E. Taglauer, *Phys. Rev. B* **19**, 1677 (1979).
- ⁶ M. Baer, *J. Chem. Phys.* **81**, 4526 (1984).
- ⁷ S. Ron, Y. Shima, and M. Baer, *Chem. Phys. Lett.* **116**, 443 (1985).
- ⁸ S. Ron, Y. Shima, and M. Baer, *Chem. Phys.* **101**, 45 (1986).
- ⁹ B. Willerding, W. Heiland, and K. J. Snowdon, *Phys. Rev. Lett.* **53**, 2031 (1984).
- ¹⁰ B. Willerding, H. Steininger, K. J. Snowdon, and W. Heiland, *Nucl. Instrum. Methods B* **2**, 453 (1984).
- ¹¹ B. Willerding, K. J. Snowdon, U. Imke, and W. Heiland, *Nucl. Instrum. Methods B* **13**, 614 (1986).
- ¹² S. Schubert, J. Neumann, U. Imke, K. J. Snowdon, P. Varga, and W. Heiland, *Surf. Sci.* **171**, L375 (1986).
- ¹³ U. Imke, S. Schubert, K. J. Snowdon, and W. Heiland, *Surf. Sci.* **189/190**, 960 (1987).
- ¹⁴ W. Heiland, U. Imke, S. Schubert, and K. J. Snowdon, *Nucl. Instrum. Methods B* **27**, 167 (1987).
- ¹⁵ J. W. Gadzuk and S. Holloway, *J. Chem. Phys.* **84**, 3502 (1986).
- ¹⁶ J. W. Gadzuk, *J. Chem. Phys.* **86**, 5196 (1987).
- ¹⁷ J. W. Gadzuk, *Surf. Sci.* **184**, 483 (1987).
- ¹⁸ S. Holloway, M. Karikorp, and J. W. Gadzuk, *Nucl. Instrum. Methods B* **27**, 37 (1987).
- ¹⁹ P. Haochang, T. C. M. Horn, and A. W. Kleyn, *Phys. Rev. Lett.* **57**, 3035 (1986).
- ²⁰ P. H. F. Reijnen, A. W. Kleyn, U. Imke, and K. J. Snowdon, *Nucl. Instrum. Methods B* **33**, 451 (1988).
- ²¹ S. Schubert, U. Imke, W. Heiland, K. J. Snowdon, P. H. F. Reijnen, and A. W. Kleyn, *Surf. Sci.* **205**, L793 (1988).
- ²² A. Danon and A. Amirav, *Phys. Rev. Lett.* **61**, 2961 (1988).
- ²³ I. S. Bitensky and E. S. Parilis, *Nucl. Instrum. Methods B* **2**, 364 (1984).
- ²⁴ I. S. Bitensky and E. S. Parilis, *Surf. Sci.* **161**, L565 (1985).
- ²⁵ M. M. Jakas and D. E. Harrison, *Surf. Sci.* **149**, 500 (1985).
- ²⁶ R. Elber and R. B. Gerber, *Chem. Phys. Lett.* **97**, 4 (1983).
- ²⁷ R. B. Gerber and R. Elber, *Chem. Phys. Lett.* **102**, 466 (1983).
- ²⁸ R. B. Gerber and R. Elber, *Chem. Phys. Lett.* **107**, 141 (1984).
- ²⁹ R. Elber and R. B. Gerber, *J. Phys. Chem.* **88**, 1571 (1984).
- ³⁰ E. Kolodney and A. Amirav, *J. Chem. Phys.* **79**, 4648 (1983).
- ³¹ E. Kolodney, A. Amirav, R. Elber, and R. B. Gerber, *Chem. Phys. Lett.* **111**, 366 (1984).
- ³² J. D. Kelley and M. Wolfsberg, *J. Chem. Phys.* **44**, 324 (1966).

- ³³D. Secrest, J. Chem. Phys. **51**, 421 (1969).
³⁴M. Attermeyer and R. A. Marcus, J. Chem. Phys. **52**, 393 (1970).
³⁵T. Ree and H. K. Shin, J. Chem. Phys. **84**, 5545 (1986).
³⁶P. J. Van Den Hoek, T. C. M. Horn, and A. W. Kleyn, Surf. Sci. **198**, L335 (1988).
³⁷H. Akazawa and Y. Murata, J. Chem. Phys. **92**, 5551 (1990).
³⁸H. Akazawa and Y. Murata, Surf. Sci. **207**, L971 (1989).
³⁹W. Lichten, J. Phys. Chem. **84**, 2102 (1980).
⁴⁰M. Barat and W. Lichten, Phys. Rev. A **6**, 211 (1972).
⁴¹K. P. Huber and G. Herzberg, *Molecular Spectra and Molecular Structure, Constants of Diatomic Molecules* (Van Nostrand Reinhold, New York, 1979), Vol. 4.
⁴²A. Danon, E. Kolodney, and A. Amirav, Surf. Sci. **193**, 132 (1988).
⁴³D. Rapp and T. Kassel, Chem. Rev. **69**, 61 (1969).
⁴⁴A. A. Abrahamson, Phys. Rev. **178**, 76 (1969).
⁴⁵C. S. Sass and J. W. Rabalais, J. Chem. Phys. **89**, 3870 (1988).
⁴⁶Y. Jo, J. A. Schultz, T. R. Schuler, and J. W. Rabalais, J. Chem. Phys. **89**, 2113 (1985).
⁴⁷M. P. D'Evelyn, A. V. Hamza, G. E. Gdowski, and R. J. Madix, Surf. Sci. **167**, 451 (1986).